variable as a function of t. The angle θ in each ply is the angle between the fiber direction and x-axis of the plate. It is also assumed that $L/h=20$ and the dwell time $\bar{T}_1=100$ where $\bar{T}_1=(E_T/\rho h^2)t_1$ with E_T denoting the modulus of a unidirectional layer transverse to the fiber direction and ρ denoting laminate density. Dynamic load factors (ratio of dynamic solution to static solution) are presented in Tables 1 and 2 for increasing values of N_0 (shown in the non-dimensional form $\bar{N}_0=N_0/E_T h$). These results correspond to $\theta=45°$ and 90° respectively. Maximum in-plane stresses for the ith layer of the laminate can be calculated from the relations‡

$$\sigma_x^i=Q_{11}^i u_x^0+z(Q_{11}^i\psi_{xx}+Q_{16}^i\psi_{y,x})$$

$$\sigma_y^i=Q_{12}^i u^0{}_{,x}+z(Q^i{}_{12}\psi_{x,x}+Q^i{}_{26}\psi_{y,x})$$

$$\tau^i{}_{xy}=Q_{16}^i u^0{}_{,x}+z(Q^i{}_{16}\psi_{x,x}+Q^i{}_{66}\psi_{y,x}) \qquad (6)$$

where Q_{ij} are the anisotropic reduced stiffnesses for plane stress. For the present plate theory in which the effects of transverse shear deformation are included the inplane stresses are not a function of w explicitly. It should not noted, however, that through the coupling of w, ψ_x, and ψ_y in the governing equations the inplane stresses are indirectly related to w. For the symmetric laminates discussed in the present work, $u_{,x}{}^0$ is a constant proportional to N_0. Thus, w, ψ_x, and ψ_y are the only time dependent variables. It should be noted that the laminates under discussion display orthotropic in-plane properties *(i.e.,* $A_{16}=A_{26}=0$) resulting in the vanishing of v^0. The interlaminar shear stress τ_{xz} can be determined by using Eqs. (6) in conjunction with the dynamic theory of elasticity in the following manner

$$\tau^i{}_{xz}=-\int_{-h/2}^{z}(\sigma^i{}_{x,x}-\rho z\psi_{x,tt})\,dz \qquad (7)$$

The dynamic load factor for the maximum value of τ_{xz} is shown in Fig. 1 for $\theta=45°$ and $z=0$. It should be noted that, depending on layer properties, the maximum value of τ_{xz} does not always occur at the laminate mid-plane. Similarly, the maximum value of the in-plane stresses does not always occur at the outer surface of the plate. It should also be noted that for $\theta=90°$, ψ_y vanishes.

A cursory examination of the numerical results reveals that an initial in-plane tensile stress resultant has considerable influence on the dynamic load factor. The exact character of the change, i.e., increase or decrease, depends on the orientation in the laminate.

References

[1] Sun, C. T. and Whitney, J. M., "Forced Vibrations of Laminated Composite Plates in Cylindrical Bending," *The Journal of the Acoustical Society of America*, Vol. 55, May 1974, pp. 1003-1008.

[2] Mindlin, R. D. and Goodman, L. G., "Beam Vibrations with Time-Dependent Boundary Conditions," *Journal of Applied Mechanics*, Vol. 17, 1950, pp. 377-380.

[3] Yu, Y. Y., "Forced Flexural Vibrations of Sandwich Plates in Plane Strain," *Journal of Applied Mechanics*, Vol. 27, 1960, pp. 535-540.

‡In general the peak values for $\psi_{x,x}$ and $\psi_{y,x}$ do not occur at the same instant. Since the numerical values for $\psi_{x,x}$ are at least ten times greater than $\psi_{y,x}$ and $Q^i{}_{11}$ and $Q^i{}_{16}$ are in the same order of magnitude, it follows that for practical applications the dynamic load factors for the inplane stresses are very close to the dynamic load factor for $\psi_{x,x}$.

Near-Field Studies of a Choked Jet Seeded with Upstream Sound

B.H.K. Lee*
National Research Council, Ottawa, Ontario, Canada

Introduction

A NUMBER of studies[1-4] on core engine noise have been published in recent years. There is substantial evidence[1,2] that the noise from low-velocity jets cannot be accounted for by Lighthill's theory alone. Internally generated noise upstream of the nozzle contributes significantly to the overall noise radiated by the jet. As early as 1953, Mawardi and Dyer[5] reported measurements on turbojet engine noise and found the velocity index to vary from 4 to 8 as the thrust was increased. The importance of internal noise has been overlooked for many years, and, in testings of jet engines, the deviation from the U^8 law was regarded as an imperfection of the engine rather than a fundamental effect.

In spite of some recent investigations by engine manufacturers and independent researchers, the subject of internal noise is still poorly understood. This is because of the complexity of the problem, and more fundamental studies are required to identify the internal noise sources, the coupling between them, and the transmission characteristics as a function of the jet flow.

To study the transmission of core noise, it is desirable to introduce sound of controllable amplitude and frequency upstream of the nozzle and to follow the development of the radiated waves and the modification by the jet flow in the near field. This paper presents some preliminary observations in the near field of a 2¼-in. cold choked jet seeded with high-intensity sound waves of discrete frequencies generated by an annular cavity cut into the inside surface of a nozzle. Microphone traverses at a frequency of 12.5 kHz have been carried out. This frequency corresponds to the fundamental of the internally generated waves, with the cavity width set at ½ in. The results for other cavity widths exhibit behavior similar to that reported herein, and detailed measurements at other frequencies are reported in Ref. 6.

Experiments

The experimental facility used in the present experiments has been described by Westley and Woolley.[7] The nozzle used in the experiments has an inside diameter D of 2.25 in. and a parallel length of 4.2 in. It was connected to a 6-in-diam air supply pipe by a converging section. Figure 1 shows a cross section of the nozzle. An annular cavity was cut on the inside surface of the nozzle at a distance $d=$ ½ in. from the exit. The cavity depth h was kept constant at ¼ in., and the width b could be varied from ⅛ to ½ in. The dimension for the nozzle wall thickness t was ⅜ in.

A ¼-in.-diam condenser microphone (B&K 4135) was mounted on a lathe bed drive and could be motor-driven at a speed of approximately 1 ips, for a distance up to 30 in. The near-field traverses of the sound pressure level at frequencies corresponding to those generated by the cavity were obtained by feeding the microphone signals through a B&K ⅓-octave frequency analyzer.

Optical studies of the jet flow and the sound field were obtained by a single-pass schlieren system with a nanolite source (model K30) and two spherical mirrors of 3-ft diam and 24-ft focal length. A microphone was used to trigger the light

Received May 22, 1975; revision received Oct. 9, 1975.
Index categories: Jets, Wakes, and Viscid-Inviscid Flow Interactions; Aircraft Noise, Aerodynamics (Including Sonic Boom).

*Associate Research Officer, National Aeronautical Establishment.

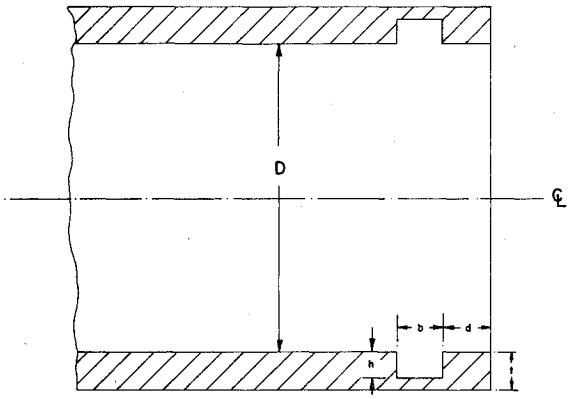

Fig. 1 Schematic of nozzle.

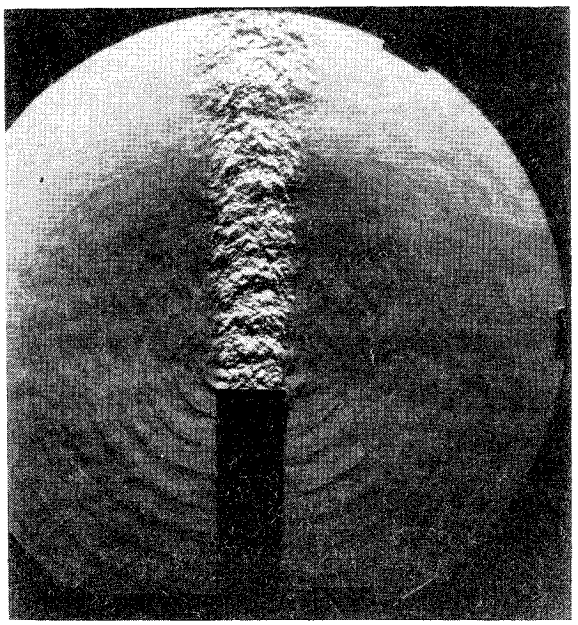

Fig. 2 Shadowgraph of the radiated sound field.

source, and single-frame photographs could be obtained at various time delays.

Results and Discussion

When a subsonic or supersonic flow passes over a cavity, an intense tone of discrete frequency sound is produced. Schlieren photographs of the acoustic field have been taken by Karamcheti[8] for flow past a rectangular cavity, and the radiation has been shown to be directional at high subsonic Mach numbers. Figure 2 shows a shadowgraph of the radiated sound field at a jet pressure ratio of 2.36. The cavity gap is ½ in. wide, and a very intense sound field can be seen. The frequency of the radiated waves is 12.5 kHz, which is calculated from the wavelength measured from the photograph. The sound waves in the downstream and forward directions are quite spherical, and they are separated by a region of poorly defined wave pattern, which is due to interactions between these two sets of waves. If the wave vectors of the two sets of waves are drawn, they will intersect on the jet boundary at a distance of approximately ½ diam downstream of the nozzle exit plane. Schlieren photographs of the cavity-generated waves inside the jet[6] show that the location of the center of the radiated waves depends on the angle made by the acoustic beam emitting from the cavity with the mean flow and roughly coincides with the point where the beam meets the jet boundary.

To study the radiation in the near field of the jet, microphone traverses of the sound pressure were made.

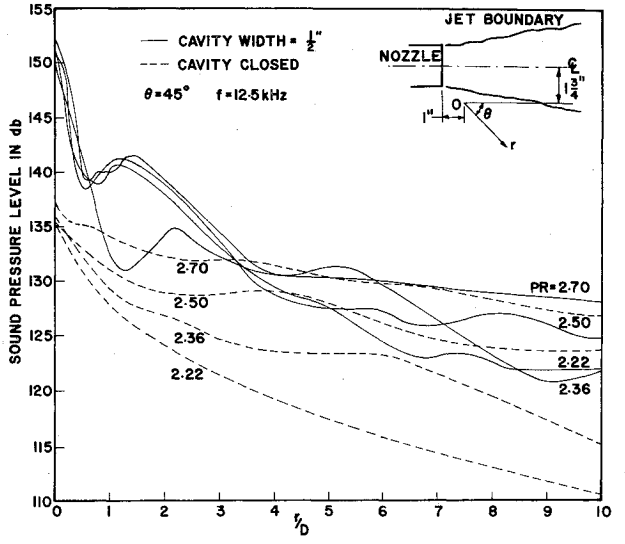

Fig. 3 Sound pressure level, dB (0.0002 dynes/cm^2), vs r/D at $\theta=45°$ with ½-in. cavity width.

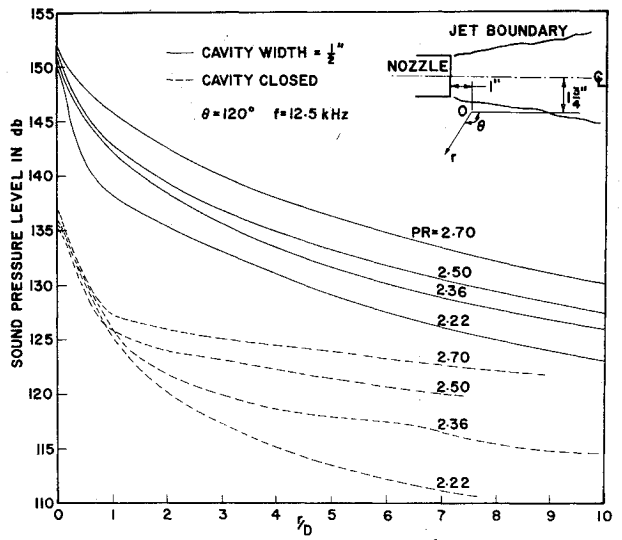

Fig. 4 Sound pressure level, dB (0.0002 dynes/cm^2), vs r/D at $\theta=120°$ with ½-in. cavity width.

Figure 3 shows the filtered sound pressure level plotted against the nondimensional distance r/D at $\theta=45°$ for the downstream set of waves. Results for four pressure ratios are given at the fundamental frequency of 12.5 kHz for the cavity-generated waves. The frequency was found to vary with the cavity width only and not with the jet pressure ratio. Corresponding to these four pressure ratios of 2.22, 2.36, 2.50, and 2.70, the pressure fluctuations on the floor of the cavity measured by a fast response transducer were 2.6, 4.3, 6, and 8.8 psi, respectively.[6] Although the correlation between these pressure measurements and the intensities of the cavity-generated waves has not been completed at this stage of the investigation, nevertheless they give an indication of the intensity of the acoustic emission which can be varied by adjusting the jet pressure ratio. The solid lines in Fig. 3 are the traverses with the cavity width set at ½ in., and the coordinate system is shown at the top right-hand corner of the figure. The origin 0 is a 1 in. downstream of the nozzle exit and 1¾ in. from the jet axis. The drop in sound pressure level with distance is very rapid for $r/D<1$, and a dip in the curves between ½ and 2 diam always is present, with that at a pressure ratio of 2.7 being the largest. To obtain an idea of the background noise, the sound pressure level is plotted in the same figure with the cavity closed, as shown by the broken

lines. The sound waves at $r/D=0$ are at least 15 dB lower than those with the cavity opened. At the highest pressure ratio of 2.7, it is seen that seeding the jet flow with intense sound waves results in a rapid decay in pressure level for a distance of 1 to 2 diam. For larger values of r/D, e.g., $r/D>5$, the effect of the cavity-generated waves is very small, whereas at the lowest pressure ratio of 2.22 the effect is quite pronounced, and the curves are separated by 10 dB or more.

The near field of the forward set of waves was studied by microphone traverses at $\theta=120°$. The sound pressure level at 12.5 kHz is plotted in Fig. 4. Comparison of this figure with Fig. 3 shows that the forward set of waves has relatively little interference from the sound field produced by the jet flow, except near the jet exit. There the nozzle exerts some influence, and the sound waves decay as spherical waves a short distance from the nozzle lip. The near field in the absence of the cavity-generated waves is shown in the same figure by the broken lines, and the intensities are substantially lower than those with the cavity width set at ½ in.

The sound pressure traverses of the downstream set of waves with the cavity closed are always higher than the forward set of waves for the four jet pressure ratios reported herein. This is to be expected, because the $\theta=45°$ traverses are closer to the noise-producing region of the jet. However, with the cavity opened, the sound pressure levels along the $\theta=120°$ traverses remains higher than the $\theta=45°$ traverses, since the drop in the sound pressure near the origin 0 is less rapid. This shows that the seeded sound has a greater influence in the forward direction, at least for this particular frequency. More experiments are needed to show whether this phenomenon is observed at other frequencies of the seeded sound waves, although traverses at 16 kHz reported in Ref. 6 show similar behavior, but the differences in the sound pressure level in the forward and downstream directions are not as large as those for 12.5 kHz.

Conclusions

Some preliminary results of the transmission of internally generated noise through a cold choked jet were presented. The sound source is an annular cavity cut into the inside surface of the nozzle. The amplitude and frequency of the cavity-generated waves can be controlled by adjusting the jet pressure ratio and the cavity width. Shadowgraphs taken of the radiated sound field show two sets of waves, one moving downstream and the other in the forward direction. They are separated by a region of poorly defined wave pattern, which is due to interactions between the two sets of waves. The radiated waves are quite spherical, and if the wave vectors of these two sets of waves are drawn, they will intersect on the jet boundary in the region where the acoustic beam emitting from the cavity leaves the jet.

Sound pressure traverses also were carried out for the downstream ($\theta=45°$) and forward ($\theta=120°$) sets of waves at a frequency of 12.5 kHz, with the cavity width set at ½ in. The $\theta=45°$ traverse shows some interference from the other noise sources in the jet such as shock cell noise, whereas the $\theta=120°$ traverse shows the waves to decay like spherical sound waves a short distance from the nozzle lip. For this particular frequency, the seeded sound waves have a larger influence in the forward direction, but more experiments are needed to show whether this is true for other frequencies as well.

References

[1]Gerend, R.P., Kumasaka, H.P., and Roundhill, J.P., "Core Engine Noise," AIAA Paper 73-1027, Oct. 1973, Seattle, Wash.

[2]Bushell, K.W., "A Survey of Low Velocity and Coaxial Jet Noise with the Application to Prediction," *Journal of Sound and Vibration*, Vol. 17, Feb. 1971, pp. 271-282.

[3]Pickett, G.F., "Core Engine Noise Due to Temperature Fluctuations Convecting Through Turbine Rows," AIAA Paper 75-528, Hampton, Va., 1975.

[4]Hock, R.G., Thomas, P., and Weiss, E., "An Experimental Investigation of the Core Engine Noise of a Turbofan Engine," AIAA Paper 75-526, Hampton, Va., 1975.

[5]Mawardi, O.K. and Dyer, I., "On Noise of Aerodynamic Origin," *Journal of the Acoustical Society of America*, Vol. 25, March 1953, pp. 389-395.

[6]Lee, B.H.K., "Transmission of Internally Generated Noise Through a Choked Jet," LTR-HA-25, 1975, National Research Council of Canada, Ottawa, Canada.

[7]Westley, R. and Woolley, J.H., "The Near Field Sound Pressures of a Choked Jet During a Screech Cycle," *Aircraft Engine Noise and Sonic Boom*, AGARD Conference Proceedings 42, May, 1969.

[8]Karamcheti, K. "Acoustic Radiation from Two-Dimensional Rectangular Cut Outs in Aerodynamic Surfaces," TN 3487, 1955, NACA.

Correlation of Vibrational-Nonequilibrium Flow in Expansion Nozzles

Kenichi Nanbu*
Tohoku University, Sendai, Japan

Introduction

MUCH work has been published on the vibrational-nonequilibrium flow in expansion nozzles.[1] Erickson[2] found numerically that the translational temperature T at large area ratios in the nonequilibrium flow calculations could be correlated as follows: the ratio of T to the temperature T_e at the same area ratio in equilibrium flow is independent of the area ratio and is given as a function of the stagnation temperature T_0 and the product $p_0\ell$, where p_0 is the stagnation pressures. The definition of ℓ follows. The purpose of this Note is to present an analytical verification of the above correlation.

Analysis and Results

We consider a pure diatomic gas flowing through a convergent-divergent nozzle with an area distribution given by

$$A/A^*=1+(x/\ell)^2 \tag{1}$$

where A is the cross-sectional area, x is the axial distance from the throat, $\ell=r^*/\tan\theta$, r^* is the throat radius, and θ is the asymptotic expansion angle. The asterisk denotes the conditions at the throat. In the range of the area ratio where vibrational freezing prevails, Eqs. (18) and (19) of Ref. 2 reduce to

$$dA/A=[(6T-5T_0')/2T(T_0'-T)]\,dT \tag{2}$$

where T is the translational temperature, and T_0' is defined by

$$T_0'=T_0+(2/7)\Theta(\sigma_0-\sigma_f) \tag{3}$$

where Θ is the characteristic temperature for vibration, $\sigma_0=[\exp(\Theta/T_0)-1]^{-1}$ is the vibrational energy at T_0, and σ is the frozen vibrational energy. Both σ_0 and σ_f are dimensionless as a result of dividing by $R\Theta$. Where R is the gas constant. The solution of Eq. (2) is

$$\frac{A}{A^*}=K\left[\frac{T}{\Theta}\right]^{-5/2}\left[1-\frac{T}{T_0'}\right]^{-1/2} \tag{4}$$

Received June 9, 1974.
Index categories: Nozzle and Channel Flow; Reactive Flows; Supersonic and Hypersonic Flow.

*Assistant Professor, Institute of High Speed Mechanics.